

SEISMIC DEMAND OF AN RC SPECIAL MOMENT FRAME BUILDING

TAEWAN KIM^{1,2} AND JINKOO KIM^{*,1}

¹*Department of Civil, Architectural and Environmental System Engineering, SungKyunKwan University, Suwon, Republic of Korea*

²*Division of Architecture, Kangwon National University, Chuncheon, Republic of Korea.*

With effect from 27th February 2008

SUMMARY

Seismic design of a building is usually performed by using a linear static procedure. However, the actual behavior of a building subjected to earthquake is inelastic and dynamic in nature, and inelastic dynamic analysis is required to evaluate the safety of the structure designed by the current design codes. In this study, an RC special moment-resisting frame building was designed by IBC 2003. Maximum plastic rotation, dissipated energy of some selected members, and the drift demand were calculated to examine whether the inelastic behavior of the building followed the intention of the design code. In addition, the effect of internal moment-resisting frames (gravity load resisting system) on resisting lateral load was investigated. According to the analysis result, the building designed by IBC 2003 showed the inelastic behavior intended in the code and satisfied the design drift limit. Copyright © 2007 John Wiley & Sons, Ltd.

1. INTRODUCTION

Most of the seismic design codes currently applied in structural design, including the International Building Code (IBC, 2003), recommend a linear static process for analysis and design. However, structures designed by seismic forces reduced by the response modification factor will behave inelastically when they are subjected to design-level earthquake. Therefore, inelastic dynamic analysis is required to evaluate the safety of the structure designed by current design codes.

Moment-resisting frames are widely used as an efficient seismic load-resisting system owing to their significant ductile behavior. Special moment frames, especially, are designed to show higher ductility. However, to design the whole structure as special moment frames may not be economical, and it is usual practice to design only perimeter frames as special moment frames. In this case the internal frames are designed to resist only gravity load (Figure 1). In reality, even though only the special moment frames located in the perimeter are designed for seismic load, internal frames also participate in resisting the seismic load. As Hueste and Wight (1997) pointed out, the interaction of the special moment frames as a ductile system and the internal frames as a non-ductile system can be important. In the SAC/FEMA project, internal frames composed of simple connections were included in the analyses, and the local collapse capacity of the internal frames affected the overall performance of buildings where the primary lateral load-resisting system was steel special moment-resisting frames (Yun *et al.*, 2002; Lee and Foutch, 2002). Kim (2004) also indicated that the premature failure of internal systems may cause an unfavorable effect on the overall stability of the structure.

In this study the seismic performance of reinforced concrete (RC) special moment frames designed per IBC 2003 was investigated. Nonlinear dynamic analyses were performed to compute the maximum

*Correspondence to: Jinkoo Kim, Department of Civil, Architectural and Environmental System Engineering, SungKyunKwan University, Suwon 440-746, Republic of Korea. E-mail: jinkoo@skku.edu

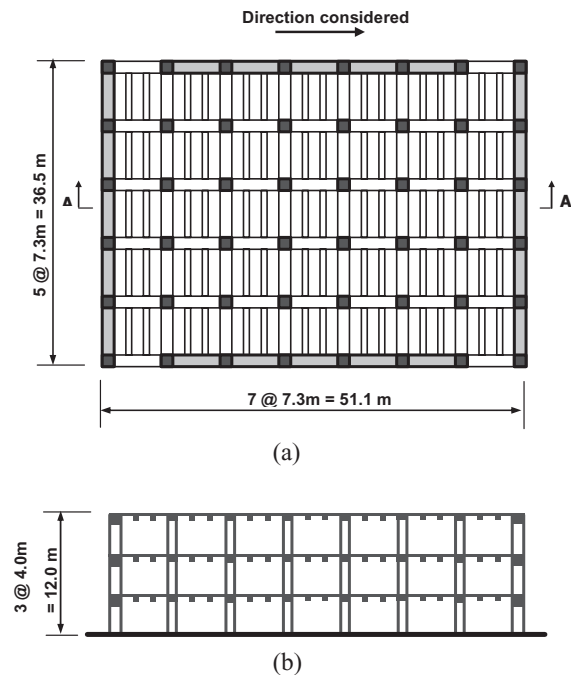


Figure 1. Model building: (a) plan; (b) section A–A'

plastic rotation, energy dissipation, and maximum inter-story drifts and to check whether the structure performed as expected. Internal frames were included in the analysis to ascertain their contribution to the lateral load-resisting capability.

2. DESIGN OF A MODEL STRUCTURE

The analysis model is a three-story RC frame structure assumed to be located in downtown Los Angeles. Structural members were designed using ACI 318 (2002), and seismic load was determined based on IBC 2003. The perimeter frames were designed as special moment frames and the internal moment frames were designed as gravity load-resisting frames. Figure 1 shows the plan and sectional view of the structure. In this study only the frames located along the horizontal direction were considered in the analysis.

2.1 Equivalent static seismic load

The lateral load-resisting system is the RC special moment frame. In this case the response modification factor (R) specified in IBC 2003 is 8 and the deflection amplification factor (C_d) is 5.5. The limit state for inter-story drift is $0.02h_{sx}$ (h_{sx} is the story height below level x) and the fundamental natural period is obtained by

$$T_a = C_t h_n^x \quad (1)$$

where C_t and x are 0.044 and 0.9, respectively, for an RC frame, and h_n is the building height. Using Equation (1), the period is computed as follows:

$$T_a = C_t h_n^x = 0.044(12)^{0.9} = 0.41 \text{ s} \quad (2)$$

The design base shear is obtained as follows:

$$V = C_s W \quad (3)$$

where W is the weight of the structure, and C_s is obtained from

$$C_s = \frac{S_{DS}}{R/I}, \leq \frac{S_{D1}}{T(R/I)} \text{ and } > 0.044 S_{DS} I \quad (4)$$

where S_{DS} and S_{D1} are the design earthquakes at short periods and 1.0 s period, respectively, and I is the occupancy importance factor. These seismic design parameters based on IBC 2003 are presented in Table 1. C_s was computed as 0.167 g by Equation (4) and the computed design base shear was 4231 kN, where the weight of the building was 25 335 kN. The calculated design base shear was distributed to each story using the equations given below:

$$F_x = C_{vx} V \quad (5)$$

$$C_{vx} = \frac{w_x h_x^k}{\sum_{i=1}^n w_i h_i^k} \quad (6)$$

where C_{vx} is the vertical distribution factor; k is an exponent related to the structure period; h_i and h_x are the height from the base to level i or x , respectively; w_i and w_x are the weight of level i and x , respectively. The calculated design lateral forces are presented in Table 2. In the design process, only half of the values in the table were used in the analysis because two identical frames are located along the direction considered.

Table 1. Seismic design coefficients for model building located in downtown LA

| | |
|-------------------------------|---|
| Maximum considered earthquake | $S_s = 1.61 \text{ g}$, $S_1 = 0.79 \text{ g}$ |
| Site class | Class D, Stiff Soil: $F_a = 1.0$, $F_v = 1.5$ |
| Design earthquake | $S_{DS} = 1.07 \text{ g}$, $S_{D1} = 0.79 \text{ g}$ |
| Seismic use group | Group II: $I = 1.25$ |
| Seismic design category | D |

Table 2. Equivalent static forces in each story

| Story | Story force (kN) | Distribution factor | Design force (kN) |
|-----------|------------------|---------------------|-------------------|
| Roof | 9187 | 0.53 | 2242 |
| 3rd story | 8075 | 0.31 | 1312 |
| 2nd story | 8075 | 0.16 | 677 |
| Sum | 25337 | 1.00 | 4231 |

2.2 Member design

Structural member design of the special moment frames was based on the ‘Chapter 21: Special Provisions for Seismic Design’ of ACI 318-02. The interior frames were designed only for gravity load. As they were also subjected to seismic load, however, seismic details were applied to retain sufficient ductility in both systems. This detailing is based on Chapter 21 of ACI 318-02, which specifies that even gravity load-resisting systems should be detailed like lateral load-resisting systems if they are simultaneously excited by an earthquake. This detailing methodology results in both systems having sufficient ductility. The only difference between the two systems is the strength against lateral loads. The resistance of the internal frame members to reverse loadings is relatively small compared to the special frame members because they are designed only for vertical load.

When the structure was designed for strength, it was observed that the maximum inter-story drift was 1.6%, satisfying the limit state of 2% of the story height specified in IBC 2003. As the design of the model building was governed by strength rather than deformation, the maximum value was much smaller than the limit value. The member size and reinforcing steel used for the perimeter and internal moment frames are presented in Tables 3 and 4, respectively.

3. ANALYTICAL MODELING

The analytical model for an RC member is composed of a linear element and two nonlinear connecting elements representing rotational degree of freedom. The member length is determined as the center-to-center distance between connections. In this analytical model, hysteretic energy is dissipated only by the nonlinear elements located at both ends of each member. For linear element, the ‘No. 2 Plastic Hinge Beam—Column Element’ in DRAIN-2DX (Prakash *et al.*, 1993) was used, and for nonlinear elements the ‘No. 10 Connection Element’ developed by Erbay *et al.* (2004) was used. Figure 2 shows

Table 3. Member size and reinforcing steel used in the exterior special moment frames

| Story | Beams | | | | | Columns | | |
|--------------|---------------------|---------------------|--------|---------------------|--------|---------------------|---------------------|---------------------|
| | Member size (mm) | Reinforcing steel | | | | Member size (mm) | Reinforcing steel | |
| | | Exterior members | | Interior members | | | Exterior members | Exterior members |
| | | Bottom | Top | Bottom | Top | | | |
| 2nd story | 560 × 760 | 8-D25 | 12-D25 | 6-D25 | 12-D25 | 660 × 660 | 16-D36* | 18-D36* |
| 3rd story | 560 × 680 | 4-D29 | 11-D25 | 4-D29 | 11-D25 | | | |
| Roof | 560 × 600 | 3-D29 | 6-D29 | 3-D29 | 6-D29 | | | |

Table 4. Member size and reinforcing steel used in the interior moment frames

| Member | Member size (mm) | Reinforcing steel |
|---------|------------------|---------------------------|
| Beams | 460 × 500 | Bottom: 5-D29, top: 3-D25 |
| Columns | 400 × 400 | 8-D25 |

the bending moment–rotation hysteresis curve for RC members. The nonlinear connection element can represent strength and stiffness degradation and pinching effects; in this research only the stiffness degradation characteristic was considered. Figure 3 shows the hysteretic behavior of the nonlinear elements (bending moment versus rotation) and the building (story shear versus inter-story drift ratio) subjected to an earthquake ground excitation. As can be observed in Figure 3(a), the stiffness of the nonlinear elements is almost infinite. Therefore, the stiffness of a member is determined only by the linear element, and the nonlinear behavior is realized by the connection elements.

Figure 4 shows two different analysis types for the nonlinear analysis in this study. Figure 4(a) is the analytical model composed only of the external special moment frame with fictitious rigid columns to consider P-delta effect (Foutch and Yun, 2002). Figure 4(b) shows the analytical model including the internal moment frame connected to the special moment frame by rigid truss elements. As the original model building is composed of two perimeter frames and four internal frames in the horizontal direction, one perimeter special moment frame and two internal frames connected in parallel are used in the analysis. Figure 4(c) shows the modeling of a typical beam–column joint where four nonlinear connecting elements are joined together.

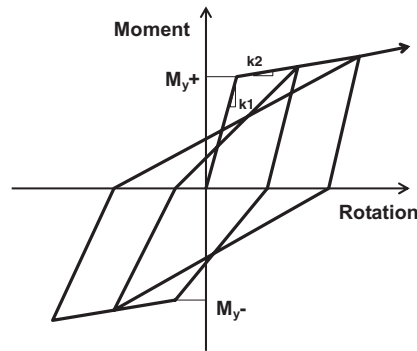


Figure 2. Hysteresis curve of RC members

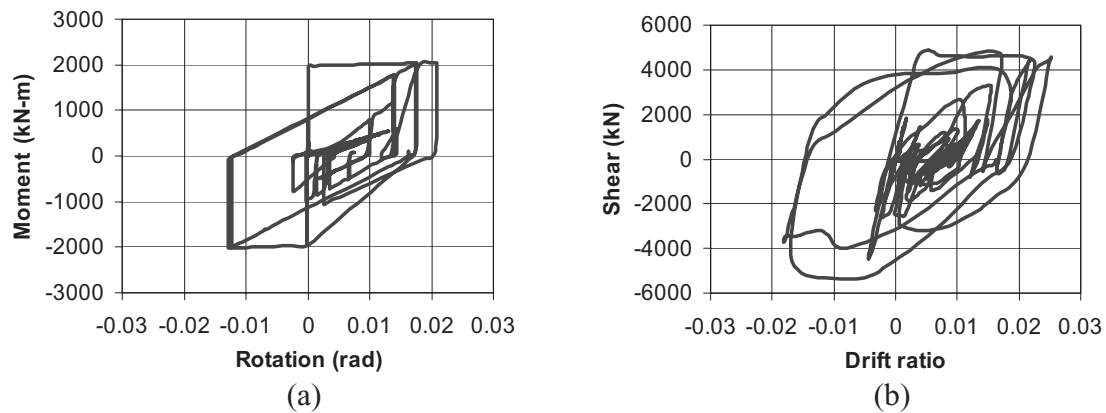


Figure 3. Hysteretic behavior of the model building: (a) bending moment versus rotation relationship of connecting members; (b) story shear versus inter-story drift ratio relationship in the first story

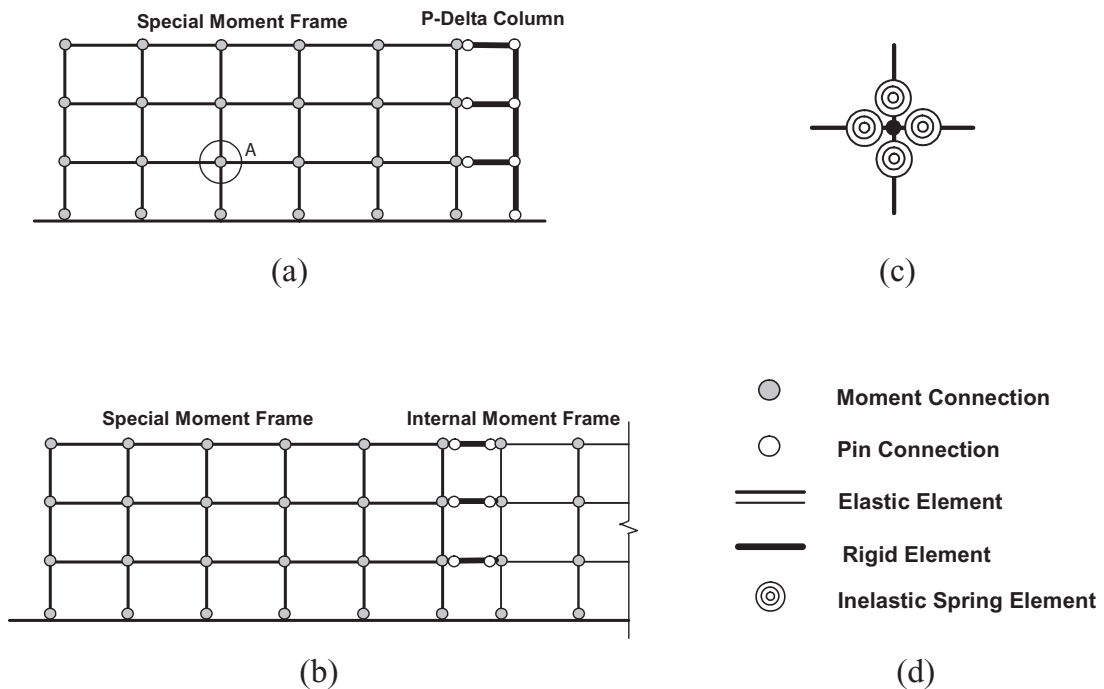


Figure 4. Analytical model for the model building: (a) special moment frame; (b) special moment frame + internal frames; (c) modeling of beam–column joints (point A in (a)); (d) legends

4. ANALYSIS RESULTS

For nonlinear time-history analyses, 20 earthquake ground motions developed for the SAC project (Somerville *et al.*, 1997) were used in the dynamic analysis. Among the records, 10 motions (LA 21 through LA 30) have a 2% probability of exceedance in 50 years (2/50) hazard level (2500-year return period) and another 10 motions (LA 01 through LA 10) have a 10% probability of exceedance in 50 years (10/50) hazard level (500-year return period). The records were modified in such a way that the spectral acceleration at the fundamental natural period becomes 1.61 *g* (maximum considered earthquake spectral response acceleration) using the method recommended in FEMA 355F (2000).

4.1 Nonlinear static pushover analysis

Figure 5 shows the base shear versus roof drift ratio relationship obtained from nonlinear static pushover analysis. The base shear of the special moment frame at the first yield turned out to be more than 50% larger than the design base shear of 2116 kN, and the maximum base shear was about twice as high as the design base shear. The strength further increased when the internal frames were included in the analysis model. It was also noted that the structure remained stable until the maximum roof displacement reached 2% of the structure height. Therefore, according to the pushover analysis, the structure has sufficient strength and ductility to resist the design-level earthquake.

4.2 Dynamic analysis

Figure 6 shows the time history of the roof story displacement when the model structure is subjected to LA 23 earthquake record. It can be observed that permanent displacement reduced significantly

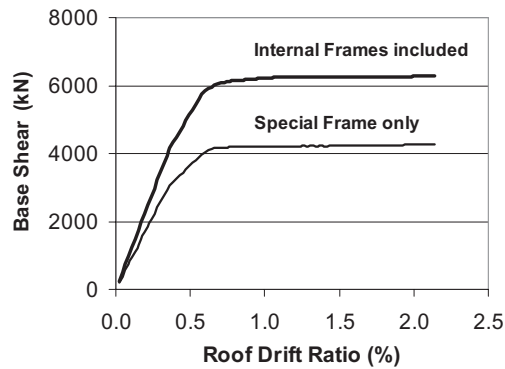


Figure 5. Base shear versus roof drift ratio relationship obtained from push-over analysis

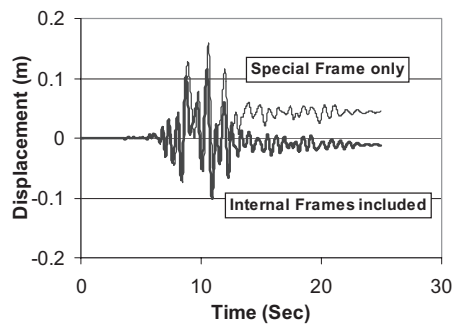


Figure 6. Time history of the roof story displacement (LA 23 earthquake)

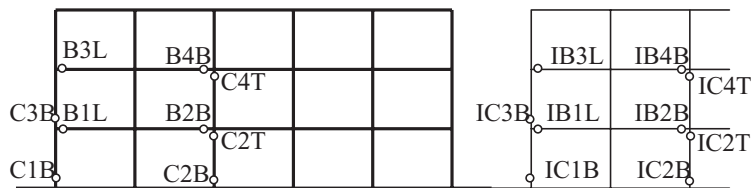


Figure 7. Location of check points

when the internal frames were included in the analysis. To observe the local behavior of the model building, various check points were assigned and their maximum plastic rotation and dissipated hysteretic energy were computed. The maximum inter-story drift was also obtained to estimate the overall damage state of the structure, and the results were compared with the UBC 94 (UBC, 1994) criterion for 10/50 hazard level as well as the IBC 2003 criterion for 2/50 hazard level.

Figure 7 shows the location of the check points: five at columns and four at beams in each of the perimeter and interior frame. Tables 5 and 6 present the mean and coefficient of variation (COV) of the maximum plastic rotation and the dissipated energy obtained from the 10 time history analysis results. It can be observed that, as expected, the maximum plastic rotation and the dissipated energy

Table 5. Maximum plastic rotation in each check point (rad)

| Analysis type: Hazard level: Variable | Special moment frame only | | | | Interior moment frames included | | | |
|---|---------------------------|------|-------|------|---------------------------------|------|-------|------|
| | 2/50 | | 10/50 | | 2/50 | | 10/50 | |
| | Mean | COV | Mean | COV | Mean | COV | Mean | COV |
| C1B | 0.020 | 0.47 | 0.004 | 0.96 | 0.020 | 0.58 | 0.003 | 1.53 |
| C2B | 0.021 | 0.46 | 0.004 | 0.96 | 0.020 | 0.57 | 0.003 | 1.48 |
| C2T | 0.000 | 2.60 | 0.000 | — | 0.001 | 1.78 | 0.000 | — |
| C3B | 0.001 | 0.00 | 0.000 | — | 0.000 | 0.00 | 0.000 | — |
| C4T | 0.001 | 2.64 | 0.000 | — | 0.004 | 0.98 | 0.000 | — |
| B1L | 0.023 | 0.40 | 0.006 | 0.52 | 0.020 | 0.53 | 0.004 | 0.83 |
| B2R | 0.021 | 0.43 | 0.006 | 0.64 | 0.017 | 0.64 | 0.004 | 1.03 |
| B3L | 0.025 | 0.42 | 0.007 | 0.27 | 0.014 | 0.72 | 0.004 | 0.61 |
| B4R | 0.023 | 0.46 | 0.006 | 0.67 | 0.013 | 0.75 | 0.004 | 0.83 |
| IC1B | — | — | — | — | 0.020 | 0.59 | 0.002 | 1.63 |
| IC2B | — | — | — | — | 0.021 | 0.57 | 0.003 | 1.46 |
| IC2T | — | — | — | — | 0.018 | 0.66 | 0.001 | 2.37 |
| IC3B | — | — | — | — | 0.001 | 1.04 | 0.000 | 2.41 |
| IC4T | — | — | — | — | 0.016 | 0.63 | 0.002 | 1.43 |
| IB1L | — | — | — | — | 0.017 | 0.62 | 0.002 | 1.48 |
| IB2R | — | — | — | — | 0.000 | 0.00 | 0.000 | — |
| IB3L | — | — | — | — | 0.009 | 0.57 | 0.001 | 1.65 |
| IB4R | — | — | — | — | 0.000 | 0.00 | 0.000 | — |

Table 6. Dissipated hysteretic energy in each check point (kNm)

| Analysis type: Hazard level: Variable | Special moment frame only | | | | Interior moment frames included | | | |
|---|---------------------------|------|-------|------|---------------------------------|------|-------|------|
| | 2/50 | | 10/50 | | 2/50 | | 10/50 | |
| | Mean | COV | Mean | COV | Mean | COV | Mean | COV |
| C1B | 110 | 0.34 | 24 | 1.05 | 107 | 0.39 | 18 | 1.37 |
| C2B | 125 | 0.34 | 28 | 1.02 | 121 | 0.37 | 21 | 1.31 |
| C2T | 2 | 2.70 | 0 | 1.77 | 3 | 1.91 | 0 | 2.14 |
| C3B | 3 | 0.00 | 0 | 0.00 | 0 | 0.00 | 0 | 0.00 |
| C4T | 3 | 2.52 | 0 | 1.29 | 12 | 1.02 | 0 | 2.27 |
| B1L | 100 | 0.31 | 35 | 0.71 | 87 | 0.34 | 27 | 1.04 |
| B2R | 86 | 0.26 | 24 | 0.77 | 75 | 0.30 | 19 | 1.14 |
| B3L | 80 | 0.43 | 31 | 0.72 | 47 | 0.42 | 18 | 1.00 |
| B4R | 78 | 0.33 | 23 | 0.87 | 40 | 0.33 | 13 | 1.08 |
| IC1B | — | — | — | — | 13 | 0.53 | 3 | 1.40 |
| IC2B | — | — | — | — | 26 | 0.51 | 4 | 1.13 |
| IC2T | — | — | — | — | 22 | 0.63 | 1 | 1.91 |
| IC3B | — | — | — | — | 3 | 0.79 | 1 | 1.08 |
| IC4T | — | — | — | — | 16 | 0.62 | 4 | 1.35 |
| IB1L | — | — | — | — | 12 | 0.60 | 2 | 1.54 |
| IB2R | — | — | — | — | 0 | 1.31 | 0 | 1.55 |
| IB3L | — | — | — | — | 4 | 0.93 | 1 | 1.99 |
| IB4R | — | — | — | — | 0 | 1.34 | 0 | 2.05 |

showed a similar trend. In the special moment frame subjected to 2/50 hazard-level earthquakes, lower ends of the first story columns (C1B, C2B) and all beams (B1L, B2R, B3L, B4R) showed a significant amount of plastic deformation. In the interior frame, the points IC1B, IC2B, IC2T (columns) and IB1L, IB3L (beams) showed inelastic deformation.

Based on these observations, the locations of plastic hinges are depicted in Figure 8. In the special moment frame, plastic hinges were formed at all lower ends of columns and at beam ends. In the interior frame, the plastic hinges were located at the lower ends of exterior columns and at all ends of interior columns. The seismic performance of the special moment frame and the interior frame showed the prototype behavior of SCWB (strong column–weak beam) and SBWC (strong beam–weak column), respectively. The special moment frame behaved as desired by the design code, but the interior frame with plastic hinges formed in columns turned out to be vulnerable to earthquake load. This shows that the internal frames deform simultaneously with the perimeter frames during an earthquake even though the interior frames are not designed for earthquake. This supports ACI 318 specifying that the gravity frames need the same seismic detailing as the lateral load-resisting frames.

The response for the 10/50 hazard-level earthquakes showed similar results with relatively smaller responses. It also can be observed in the tables that when the internal frame was included the plastic rotation and dissipated energy of beams in the special moment frame were reduced compared to when the internal frames were not included. When only the special moment frame was analyzed, the maximum plastic rotation of beams was almost uniform throughout the stories. When the internal frames were included, however, the beam plastic rotation in the third floor (B3L, B4R) of the special moment frame reduced more than that in the second floor (B1L, B2R). This indicates that the participation of internal frames reduces the seismic response of the primary seismic load-resisting system. The COV of the maximum plastic rotation was less than 0.5 when only the special moment frame was analyzed, whereas it was larger than 0.5 when the interior frames were included. This is due to the interaction between the two systems with different collapse mechanisms. Therefore it can be concluded that when only the perimeter frame is considered in the seismic analysis the reliability of the analysis results may be overestimated. This indicates that the interior gravity frames need to be included in the seismic analysis.

Table 7 and Figure 9 show the maximum inter-story drift ratios for the 2/50 and 10/50 events, where it can be observed that the inclusion of the interior frames contributed to the inter-story drift ratio significantly. When only the perimeter frame was analyzed for the 2/50 hazard-level earthquakes, the inter-story drifts of the second and third stories were larger than that of the first story. When the interior frames were included in the analysis, however, the inter-story drift decreased significantly in the higher stories. This is due to the fact that the interior frames were designed with the same sized members throughout the stories even though the story shear was smaller in the higher stories. However, there was no significant reduction in the maximum inter-story drift ratio; it reduced slightly from 2.88%

Table 7. Seismic demand for the mean maximum inter-story drift ratio (%)

| Analysis type: Hazard level: Story | Special moment frame only | | | | Internal moment frames included | | | |
|--|---------------------------|------|-------|------|---------------------------------|------|-------|------|
| | 2/50 | | 10/50 | | 2/50 | | 10/50 | |
| | Mean | COV | Mean | COV | Mean | COV | Mean | COV |
| 1 | 2.63 | 0.36 | 0.96 | 0.39 | 2.47 | 0.47 | 0.76 | 0.53 |
| 2 | 2.88 | 0.36 | 1.07 | 0.28 | 2.29 | 0.45 | 0.81 | 0.41 |
| 3 | 2.85 | 0.39 | 0.89 | 0.36 | 1.53 | 0.45 | 0.60 | 0.39 |

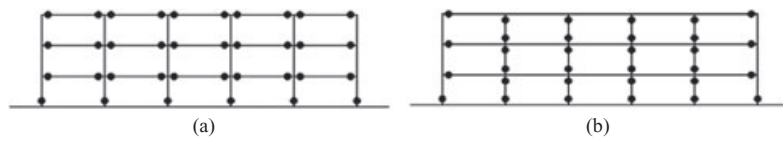


Figure 8. Location of plastic hinges: (a) perimeter special moment frame; (b) internal moment frame

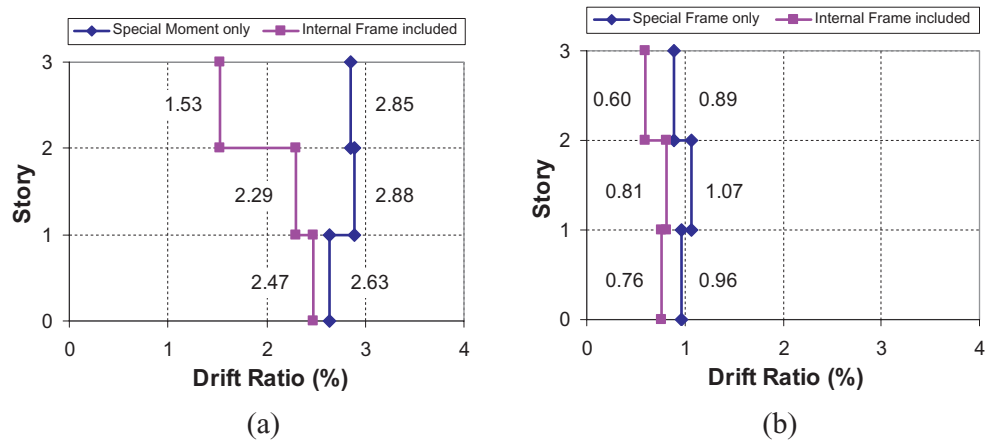


Figure 9. Mean maximum inter-story drift demand: (a) 2/50 hazard level; (b) 10/50 hazard level

to 2.47%. These maximum inter-story drift ratios are within the 2% allowable inter-story drift ratio prescribed in IBC 2003 for 2/3 of the 2/50 hazard-level events. In the case of 10/50 hazard-level earthquakes, the inter-story drifts decreased slightly in all stories; however, the overall trend was the same. The maximum inter-story drift ratio slightly decreased from 1.07% to 0.81%, in which the structure behaved almost linearly. According to the pushover analysis results shown in Figure 5, the first yielding occurred at the inter-story drift of 0.3%, which corresponds to the displacement at the design base shear. Full yielding occurred at the inter-story drift of 0.6%. Considering that the maximum inter-story drift obtained from dynamic analysis with 10/50 events is less than 1.0%, the ductility demand is less than 1.7 (1.0/0.6). Therefore, the structure will experience minute plastic deformation when subjected to earthquakes with a return period of 500 years. This coincides with the small maximum plastic rotation shown in Table 5. Similarly to the maximum plastic rotation and the energy dissipation, the COV of the maximum inter-story drift ratio increased when the interior frames were included in the analysis.

5. CONCLUSIONS

Seismic performance of a three-story RC frame building designed per IBC 2003 was investigated through nonlinear static and dynamic analyses. The effect of interior moment frames on various seismic demand parameters was also studied. The findings of the study are summarized as follows:

1. The seismic performance of the special moment frame and the interior frame showed the prototype behavior of strong column–weak beam and strong beam–weak column, respectively.

2. The seismic response of the structure turned out to meet the performance requirements of the IBC 2003 for 2/3 of 2/50 hazard-level earthquakes. For 10/50 hazard-level earthquakes the structure experienced minute inelastic deformation.
3. When the internal frames were included in the seismic analysis, the decrease in plastic rotation and energy dissipation of columns was not significant compared to when only the exterior special moment frame was considered; however, the reduction was large in beams. Also the demand for the maximum inter-story drift did not decrease significantly, but the reliability of the analysis results decreased due to the participation of the internal frames. Therefore the internal frames designed only for gravity load as well as the perimeter frames designed for seismic load need to be included in the analysis to investigate the seismic performance of RC framed structures.

ACKNOWLEDGEMENT

This work was supported by the Basic Research Program of the Korea Science & Engineering Foundation (Grant No. M10600000234-06J0000-23410). The authors appreciate this financial support.

REFERENCES

- ACI 318. 2002. *Building Code Requirements for Structural Concrete (ACI 318-02) and Commentary (ACI 318R-02)*. American Concrete Institute: Farmington Hills, MI.
- Erbay ÖO, Yun S-Y, Foutch DA, Aschheim MA. 2004. UIUC extensions to the library of elements for DRAIN-2DX. Paper no. 2530, *13th World Conference on Earthquake Engineering*, Vancouver, BC, Canada.
- FEMA 355F. 2000. *State of the Art Report on Performance Prediction and Evaluation of Steel Moment-Frame Buildings*. Federal Emergency Management Agency: Washington, DC.
- Foutch DA, Yun S-Y. 2002. Modeling of steel moment frames for seismic loads. *Journal of Constructional Steel Research* **58**: 529–564.
- Hueste MBD, Wight JK. 1997. Evaluation of a four-story reinforced concrete building damaged during the Northridge earthquake. *Earthquake Spectra* **13**(3): 387–414.
- IBC. 2003. *International Building Code*. International Code Council: Falls Church, VA.
- Kim T-W. 2004. Performance assessment of reinforced concrete structural walls for seismic loads. PhD dissertation, University of Illinois at Urbana-Champaign, Urbana, IL.
- Lee K, Foutch DA. 2002. Seismic performance evaluation of pre-Northridge steel frame buildings with brittle connections. *Journal of Structural Engineering* **128**(4): 546–555.
- Prakash V, Powell G, Campbell S. 1993. DRAIN-2DX base program description and user guide: version 1.10. *Report no. UCB/SEMM 93/17 and 93/18*. Department of Civil Engineering: University of California, Berkeley, CA.
- Somerville P, Smith N, Puntamurthula S, Sun J. 1997. Development of ground motion time histories for phase 2 of the FEMA/SAC steel project. *Report no. SAC/BD 97/04*. SAC Background Document, SAC Joint Venture: Richmond, CA.
- UBC. 1994. *Uniform Building Code*. International Conference Building Officials: Whittier, CA.
- Yun S-Y, Hamburger RO, Cornell CA, Foutch DA. 2002. Seismic performance evaluation for steel moment frames. *Journal of Structural Engineering* **128**(4): 534–545.